Transactions of the Korean Nuclear Society Autumn Meeting
Changwon, Korea, October 24-25, 2024

Nanodosimetry around the Metal Nanoparticle: A Monte Carlo Study

Taeyun Kim [a], Rodrigo Hernández Millares [a], Taewan Kim [a], Mingi Eom [a], Jiwon Kim [a], Sung-Joon Ye [a,b,c,d*]
[a]*Department of Applied Bioengineering, Graduate School of Convergence Science and Technology, Seoul National University, Seoul, 08826, Republic of Korea*
[b]*Research Institute for Convergence Science, Seoul National University, Seoul, 08826, Republic of Korea*
[c]*Advanced Institute of Convergence Technology, Seoul National University, Suwon, 16229, Republic of Korea*
[d]*Biomedical Research Institute, Seoul National University Hospital, Seoul, 03080, Republic of Korea*

[*]*Corresponding author: sye@snu.ac.kr*

1. Introduction

Metal nanoparticles (MNPs) labeled with radioisotopes (RIs) are employed as radio-enhancers due to their capacity to increase the radiation dose in their immediate surroundings. Various MNP materials, including gold, platinum, hafnium oxide, and iron oxide, have been investigated for their potential radio-enhancement effects. Among these, gold nanoparticles (AuNPs) have been the subject of extensive research due to their distinctive properties such as biocompatibility, utility as imaging contrast agents, and ease of functionalization with different biomolecules [1, 2, 3, 4].

A comprehensive understanding of dosimetry at the nanoscale is crucial for optimizing the use of MNPs. Monte Carlo (MC) simulations are commonly employed to estimate dose distributions at nano- or micrometer scales, and recent advances in computational power have enabled the tracking of individual electrons down to energies as low as 10 eV, providing highly detailed insights into dose deposition at this scale. This study seeks to shed light on the radio-enhancement effects of MNPs by clarifying the nanodosimetry around MNPs labeled with RIs using MC simulations.

2. Materials and Methods

2.1 Monte Carlo simulation

A 50 nm-diameter NP of silver (Ag) core and Au shell (Ag@Au NP) was modeled using both MCNP6.2 and Geant4. Auger-emitting RIs (^{103}Pd and ^{131}Cs), as well as mono-energetic electrons or photons (3, 5, 10, and 30 keV), were adsorbed onto the 10 nm radius Ag core, which was then encapsulated within a 15 nm thick Au shell. The dose enhancement factor (DEF) by Au shell was determined by calculating the radial dose distribution at intervals ranging from 5 to 1,000 nm, extending up to a distance of 1 mm from the spherical shell of water surrounding the Ag@Au NP.

In MCNP6.2, the physics library eprdata 14, which is based on EPICS 2014, was used. For Geant4, version 11 was employed, utilizing Geant4-DNA physics for the cross-section data of Au and water. For the Ag core, the Livermore physics was applied. Both MC codes were configured with an energy cutoff of 100 eV for photons and electrons, employing a single electron transport method.

3. Results and Discussion

3.1 Radial dose distribution

Fig. 1 shows the radial dose distributions and DEFs for mono-energetic electrons. At 3 and 5 keV, there was a notable difference between the results produced by both MC codes, particularly when an Au shell was present, where the discrepancy was more pronounced. As the electron energy increased, the differences between MCNP6.2 and Geant4 diminished. When a water shell was present, the results from both MC codes were nearly identical. However, with an Au shell, MCNP6.2 calculated higher radial dose values than Geant4 at distances within 100 nm.

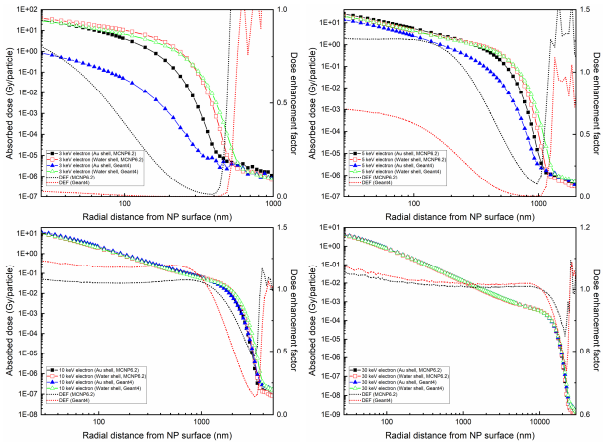

Fig. 1. Radial dose distribution and dose enhancement factor of mono-energetic electrons.

Fig. 2 shows the radial dose distributions and DEFs for mono-energetic photons. Similar to the case with electrons, a significant difference between both MC codes was observed at 3 and 5 keV in the presence of an Au shell. However, this difference gradually diminished as the photon energy increased. Notably, with an Au shell, MCNP6.2 consistently produced larger radial dose values than Geant4 within 100 nm, which is the same trend as that observed for the electrons. In the DEF of 5, 10, and 30 keV photons, clear peaks were observed.

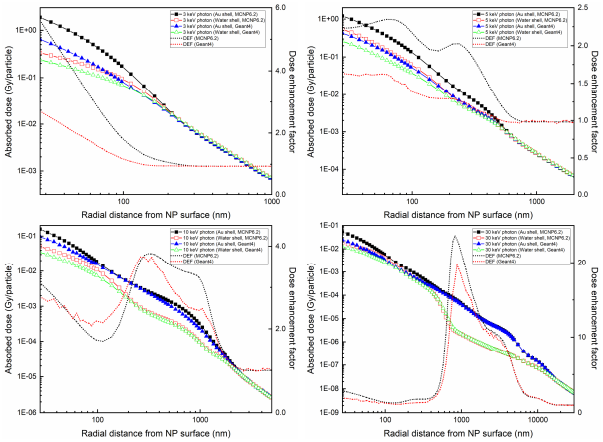

Fig. 2. Radial dose distribution and dose enhancement factor of mono-energetic photons.

Fig. 3 shows the radial dose distributions and DEFs of ^{103}Pd and ^{131}Cs. In the presence of an Au shell, the difference between both MC codes is most pronounced within the first few hundred nanometers, where MCNP6.2 also yields a higher DEF compared to Geant4. When with a water shell, the difference is relatively minor. Beyond this region, both codes produce very similar radial dose values, regardless of whether an Au or water shell was presented.

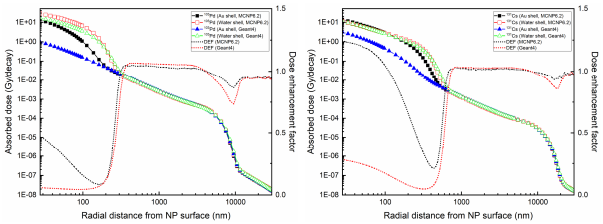

Fig. 3. Radial dose distribution and dose enhancement factor of ^{103}Pd and ^{131}Cs.

4. Conclusions

We conducted a nanodosimetry around an Ag@Au NP using both MCNP6.2 and Geant4. Apart from the results at 3 and 5 keV, both MC codes obtained similar radial dose distribution and DEF. The discrepancies at these low energies are primarily due to the different cross-section data for low-energy electrons used by MCNP6.2 and Geant4-DNA physics. Both ^{103}Pd and ^{131}Cs were observed to have negligible dose enhancement. This is expected because the radial dose of electrons is much larger than that of photons, as observed in the radial dose distributions of electrons and photons, so the dose enhancement by photons is expected to be neglected. In the future, nanodosimetry studies will be conducted using other promising RIs, such as ^{166}Ho [5, 6].

Acknowledgements

This work was supported by the National Research Foundation of Korea (NRF) grant funded by the Korea government (MSIT) (No. RS-2023-00237149).

REFERENCES

[1] S. Jung, T. Kim, W. Lee, H. Kim, H.S. Kim, H.J. Im, and S.J. Ye, Dynamic in vivo X-ray fluorescence imaging of gold in living mice exposed to gold nanoparticles, IEEE Trans. Med. Imaging., Vol. 39, p. 526–533, 2019.
[2] S. Jung, J. Lee, H. Cho, T. Kim, and S.J. Ye, Compton background elimination for in vivo x-ray fluorescence imaging of gold nanoparticles using convolutional neural network, IEEE Trans. Nucl. Sci., Vol. 67, p. 2311–2320, 2020.
[3] T. Kim, W. Lee, M. Jeon, H. Kim, M. Eom, S. Jung, H.J. Im, and S.J. Ye, Dual imaging modality of fluorescence and transmission X-rays for gold nanoparticle-injected living mice, Med. Phys., Vol. 50, p. 529–539, 2023.
[4] T. Kim, R.H. Millares, T. Kim, M. Eom, J. Kim, and S.J. Ye, Nanoscale dosimetry for a radioisotope-labeled metal nanoparticle using MCNP6.2 and Geant4, Med. Phys., In press, 2024.
[5] T. Kim, B.Y. Han, S. Yang, J. Lee, G.M. Sun, B.G. Park, and S.J. Ye, Thermal-hydraulic safety analysis of radioisotope production in HANARO using MCNP6 and COMSOL multiphysics: A feasibility study, Nucl. Eng. Technol., Vol. 55, p. 3996–4001, 2023.
[6] T. Kim, B.Y. Han, S. Yang, J. Lee, G.M. Sun, B.G. Park, and S.J. Ye, Systematic analysis for the thermal stability assessment of ^{166}Ho production using HANARO: An in silico study, Nucl. Eng. Technol., In press, 2024.